

High-Performance Lithium Polymer Battery Pack for Real-World Racing Motorcycle

Seyedreza Azizighalehsari¹ Prasanth Venugopal¹ Deepak Pratap Singh² Mark Huijben²
Jelena Popovic¹ Braham Ferreira¹

¹Power Electronics and EMC group, University of Twente, Enschede, The Netherlands

²Inorganic Materials Science group, University of Twente, Enschede, The Netherlands.

E-Mail: s.azizighalehsari@utwente.nl

URL: <https://www.utwente.nl/>

Acknowledgments

We thank the Electric Superbike Twente team to provide the Lithium Polymer cells and Kevin Schonewille the power train engineer of the team for the contribution.

Keywords

«Batteries», «Battery Impedance Measurement», «Energy storage», «Electric Vehicle»

Abstract

This paper deals with the qualification testing to design a battery pack for a fully electric racing motorcycle. To obtain the best performance from the cells and considering the point that in this case the battery pack will be used in special racing condition, finding the best configuration and cells sequence to be connected together in that's configuration is very important to make the battery pack. To avoid impedance mismatching inside the modules and the final pack, electrochemical impedance spectroscopy, capacity test, and impulse current test has been used to select appropriate cells to be connected in strings and make a uniform and high-performance battery pack with the best configuration based on the categorized cells. Experimental results obtained from the cell to cell variation and also impedance measurement for each module prove the uniformity in impedance.

Introduction

Battery in energy storage applications such as electric vehicles (EVs), railway transportation systems, renewable energy systems, and smart grids, etc. is a key component and very critical functional subsystem [1], Due to this reason, it is not a long stretch to consider battery systems as a heart for the energy storage system. These days, lithium-ion batteries (LIBs) due to their excellent performance in energy density, power density, lifetime, and columbic efficiency are the most favorable technology in energy storage systems, in comparison with the lead-acid, nickel-metal hydride, and nick-cadmium batteries, in order to satisfy the increasing market demand [2] [3].

One of the main development criteria in LIBs for use in EVs is the specific energy as part of the approach to increase the driving range. LIBs that are commercially available cover a broad range of specific energy from 100 to 200 Wh/kg that in comparison with the lead-acid batteries remain far above their specific energy, which is around 50 Wh/kg [4]. This advantage has resulted in a general upward tendency to use these batteries as the most appropriate energy storage system in EVs [2].

Ref [5] made a comprehensive comparison between different kinds of batteries in terms of energy and specific density that LIBs and lithium-polymer (Li-PO) exhibit the best energy density (Wh/kg) and specific density (Wh/l). Li-PO batteries are a kind of Li-ion batteries with the main difference between these two types in the chemical electrolyte between their positive and negative electrodes. A Li-ion battery (LIB) is composed of a liquid electrolyte while a Li-Po battery is made of a solid polymer electrolyte instead. The polymer may be a solid or a semi-solid (gel)[6]. The polymer electrolyte provides more stable performance under vibration conditions for the lithium polymer batteries [7] Li-Po batteries because of their ability to be made in small-scale size and different thicknesses and being lighter than other types of LIBs can be used in different special small portable applications where these

parameters are important. Low self-discharge rate in Li-Po batteries [8] is another advantage that makes these types of batteries more useable for applications that will remain unused for several days.

This paper is organized as follows, In section II Li-Po cells and their advantages to be used in different applications are introduced. In section III Electrochemical Impedance Spectroscopy as an approach to sort the cells according to their spectrum from low frequency to high frequency has been discussed. In section IV a second-order model proposed for Li-Po cells and the model parameter have been measured by DC impulse approach, in section V to verify the method that has been used for cell sorting and matching, the battery capacity test is done for four selected cells from each different group. Finally, the battery pack configuration and conclusion are discussed.

Lithium-Polymer Batteries

Li-Po batteries as a modified type of LIBs due to their exceptional advantages like high power density, low self-discharge rate, reduced thickness, fast discharge capability, flexibility, and less weight can be an interesting choice in different applications.

The application in this study is a fully electric racing motorcycle and because of its special condition and the requirement for a racing application, the battery pack should have the capability to dispense a large amount of instantaneous power and also be as light as possible to increase the vehicle performance during the race. A battery pack with 710 V terminal voltage and 19.05 Ah capacity is constructed by 576 Li-Po cells. The main characteristics of the cells are resumed in Table 1.

Table1: Key features of the cell under the test based on the datasheet

Characteristics	Unit	Value
Nominal Capacity	Ah	≈ 6.3
Nominal Voltage	V	3.7
Maximum voltage	V	4.2
Minimum Voltage	V	3.0
Maximum continues charge current	A	12.7
Maximum continues discharge current	A	127.0

To build the battery pack the first challenge is to assess all cells and check the manufacturer's claim about the cell capacity and internal resistance. In addition, to assemble the cells in battery module and pack it is important to categorize the cells according to their impedance to avoid impedance mismatching and the issues that come with impedance imbalance in battery pack.

Electrochemical Impedance Spectroscopy

Electrochemical Impedance Spectroscopy (EIS) is a powerful technique that has been used to evaluate the battery system performance, the main difference between EIS technique with other techniques is that in this method the impedance is measured in the frequency domain instead of the time domain. Battery resistance, capacitance, and inductance can be measured with EIS analysis by injecting an AC sweep signal and monitoring the response [9]. EIS technique can be implemented in two different ways, in the first method voltage signal is injected and current response is measured, This is called potentiostatic electrochemical impedance spectroscopy (PEIS), while in the second method the input signal is current and the impedance spectroscopy is extracted by measuring the voltage response. This is called galvanostatic impedance spectroscopy.

The potentiostatic method has been chosen in this case because in the galvanostatic method even a small change in current amplitude will be led to high variation in voltage response and it is not easy to obtain a linear response.

A wide spectrum from low to high frequency to check the impedance of the cells before assembling them in series and parallel for all Li-Po cells is done by BioLogic's VMP-300. The response in high-frequency measures the equivalent series resistance of the cell, and in low-frequency, measures the short-term and long-term transient response of the cells. According to Fig.1 that shows the EIS results for some randomly selected cells with the frequency range of 1 Hz till 1kHz, the majority of the cells have the same Nyquist plot. The cells with significant variation from other cells in their Nyquist plot are considered as unused cells to avoid mismatch and improve the battery pack performance. In addition,

the cells have been sorted and then categorized into different groups according to their internal resistance.

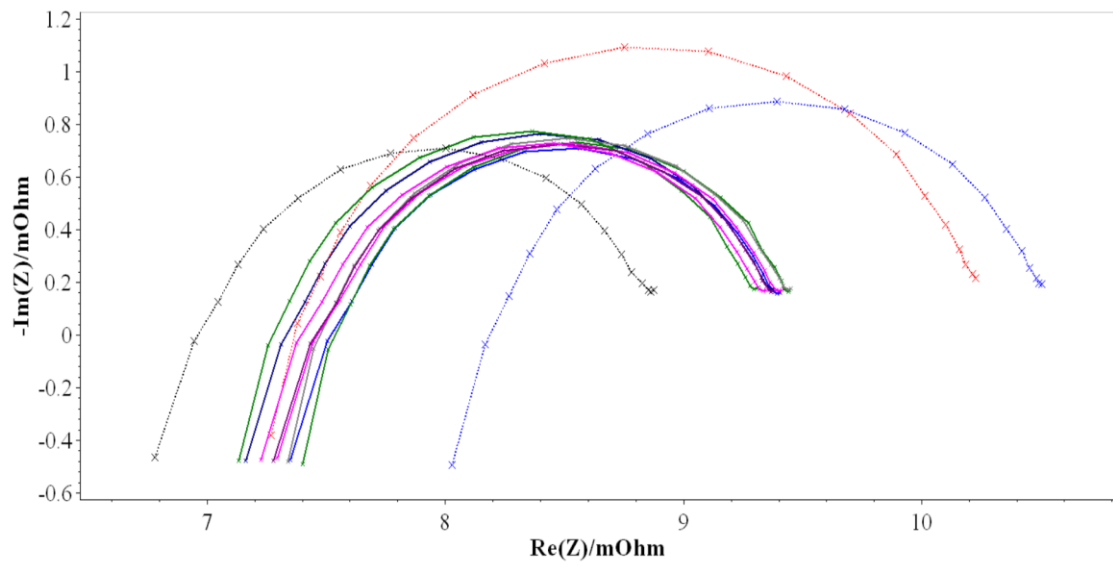


Fig. 1: EIS results in Nyquist form for some randomly selected Li-Po cells after formation cycling in the same SOC

After the first cell screening step and remove the outlier cells with the most variation in their internal parameters, all the cells have been sorted according to their internal resistance and been categorized into three different groups, the group with the lowest (Z1), middle (Z2), and highest (Z3) impedance as shown in Fig. 2.

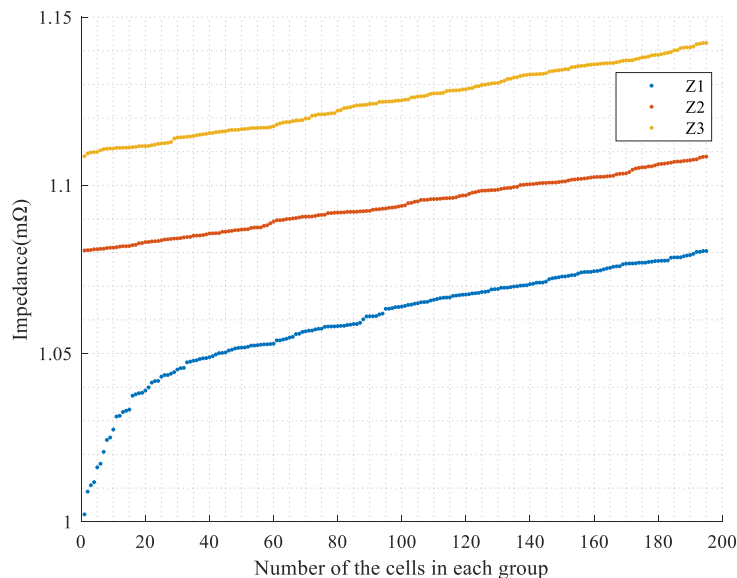


Fig.2: Cell categorization according to their internal resistance into three groups

Electrical Modeling of Cells

It is crucial to fine-tune the equivalent circuit model (ECM) for each cell and perform an analysis of the model parameter according to the cell performance. Fig. 3 illustrates a second-order ECM that in ref [12] this model introduced as a high accurate model between different ECM. In all of the ECM, there are three important elements, the open circuit voltage (OCV), series resistance (R_s), and the RC network that model diffusion voltages [13]. As the number of parallel RC networks is higher in an ECM, it can improve the accuracy of dynamic battery response prediction [14].

DC pulse approach as the most used method to measure the impedance and model parameter has been used to measure and calculate the selected Li-Po cells model parameters [15]. The measurement

approach is uncomplicated and easy to do by applying a current pulse (ΔI) to the cell and measuring the resulting change in the voltage (ΔV); the impedance of the battery (R) is obtained by dividing the voltage change by the current change.

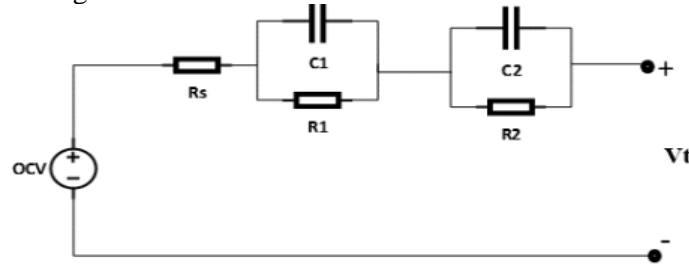


Fig. 3: Battery second-order equivalent circuit model

To calculate the model parameters of the Li-Po cells with the DC impulse current method each parameter can be extracted by measuring the voltage drop according to the current pulse in different points. The parameters have been calculated according to the ref [15],[16] The first parameter is the equivalent series resistance (R_s) that can be achieved by measuring the voltage drop that happens immediately after applying DC impulse current (V_{1s}). For the next two RC networks parameters that are used to model the battery transient state, the R_1C_1 and R_2C_2 branches are corresponding to the short-term and long-term transient response of the cell respectively. The voltage variation related to the short and long term transient have been illustrated in Fig. 4.

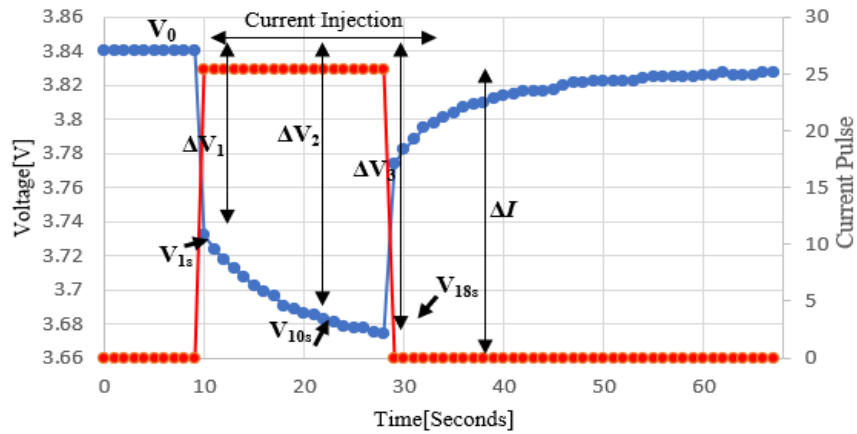


Fig. 4: voltage variation in current pulse approach method to model Li-Po cell

According to figure 4, each parameter can be defined as the following equations :

$$R_s = \frac{V_{1s} - V_0}{\Delta I}, \quad R_1 = \frac{V_{10s} - V_{1s}}{\Delta I}, \quad R_2 = \frac{V_{18s} - V_{10s}}{\Delta I} \quad (1)$$

The value of capacitance C_1 and C_2 for each Li-Po cell have been calculated according to references [16], [17].

$$C_1 = \frac{(t_2 - t_1)}{R_1 * \ln\left(\frac{V_{10s}}{V_{1s}}\right)}, \quad C_2 = \frac{(t_3 - t_2)}{R_2 * \ln\left(\frac{V_{18s}}{V_{10s}}\right)} \quad (2)$$

In these equations, V_{1s} is the instantaneous voltage dropping immediately after applying impulse current that in this case according to the measuring sampling rate it has been considered the voltage value after $t_1=1$ second. Also, V_{10s} and V_{18s} are the voltage value after 10 and 18 seconds. Fig. 5 illustrates the voltage variation after applying DC impulse current in different C_{rate} for cell #1. This approach has been done for all selected cells and the model parameters are calculated in different C_{rate} according to their voltage variation during the current pulse injecting.

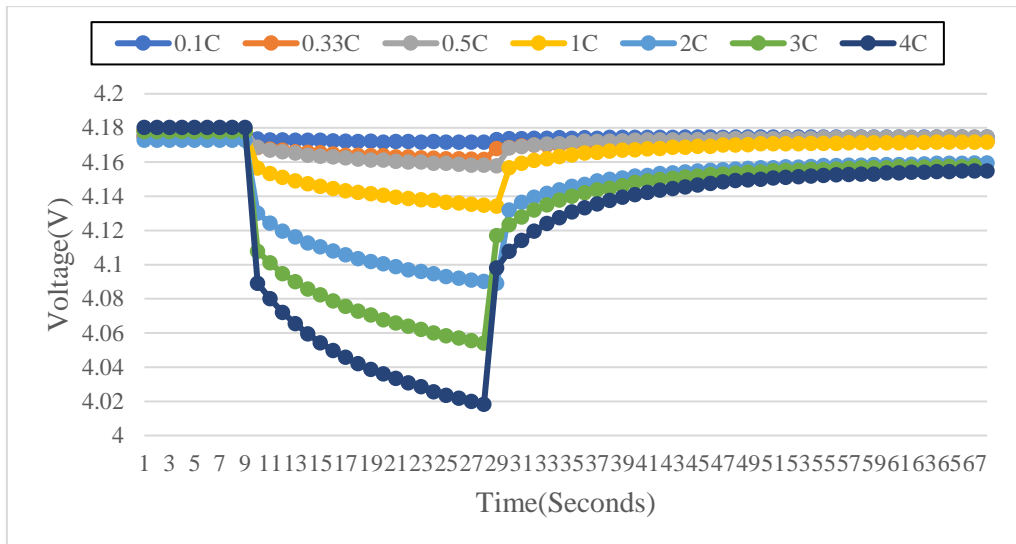


Fig. 5: Voltage variation in current pulse approach method to model Li-Po cell in different C rate for cell#1

The model parameter calculation has been done based on voltage variation measurement for selected cells and the average equivalent series resistance in different C_{rate} is $3.46\text{ m}\Omega$. Fig. 6 illustrates the histogram bar for the equivalent series resistance base on EIS measurement that for the majority of the cells, the R_s is $1.1\text{ m}\Omega$.

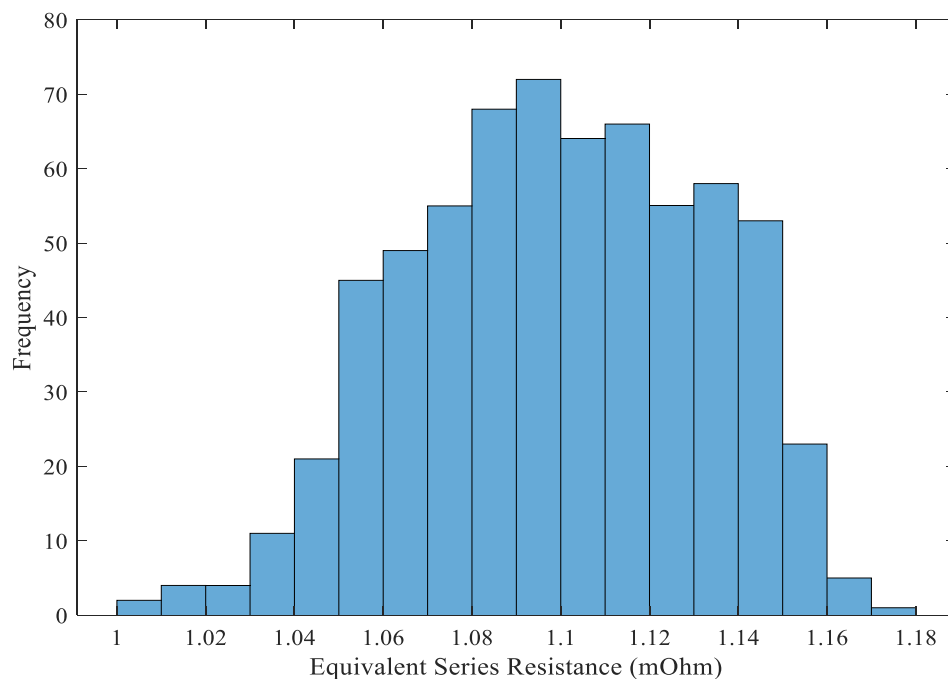


Fig. 6: Histogram bar for the equivalent series resistance base on EIS measurement for all 600 cells

Battery Capacity Test

Verifying the cell datasheet claims by measuring battery capacity during battery charge and discharge in special condition is the first aim of the battery capacity test, also verify the classification method that was done for all the cells is the second aim of doing capacity test by selecting 1 cell from each group and 1 cell from the outlier cells group. The general approach of this test is simple, by subjecting the cells in different discharge rate conditions and measure the battery capacity and energy content as a function of C_{rate} . The cells have been charged in the same situation according to the manufacture's datasheet in a standard cycle. The results of the capacity test for these 4 cells in different C_{rate} are shown in Fig. 7 and Fig. 8.

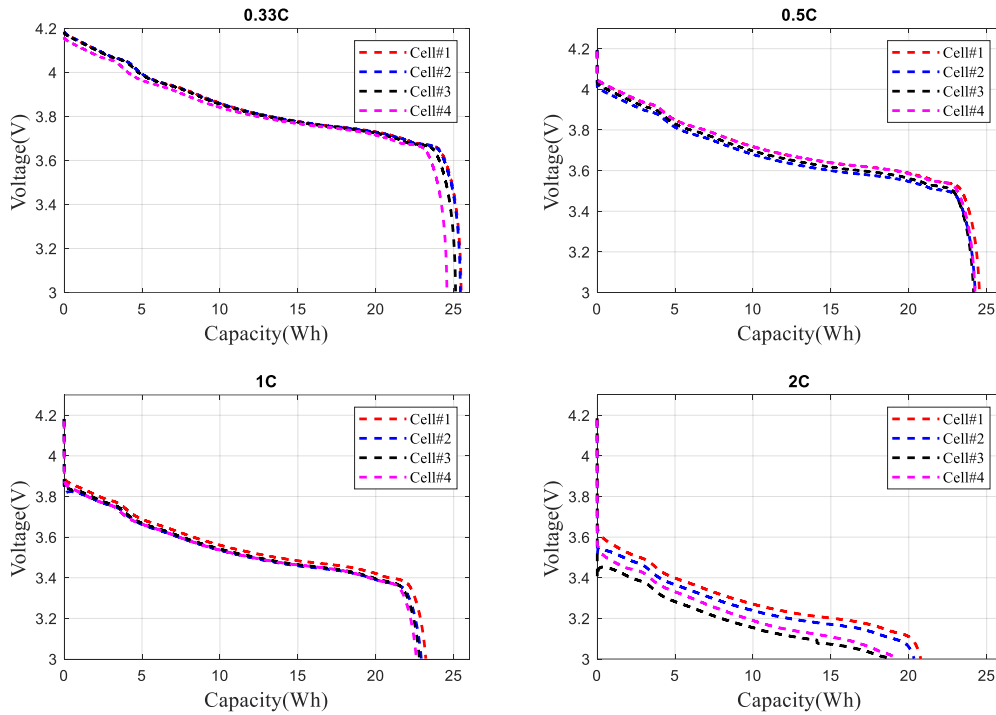


Fig. 7: Voltage vs Capacity during the capacity test for selected cells in four different C_{rate} (Temperature 21°C)

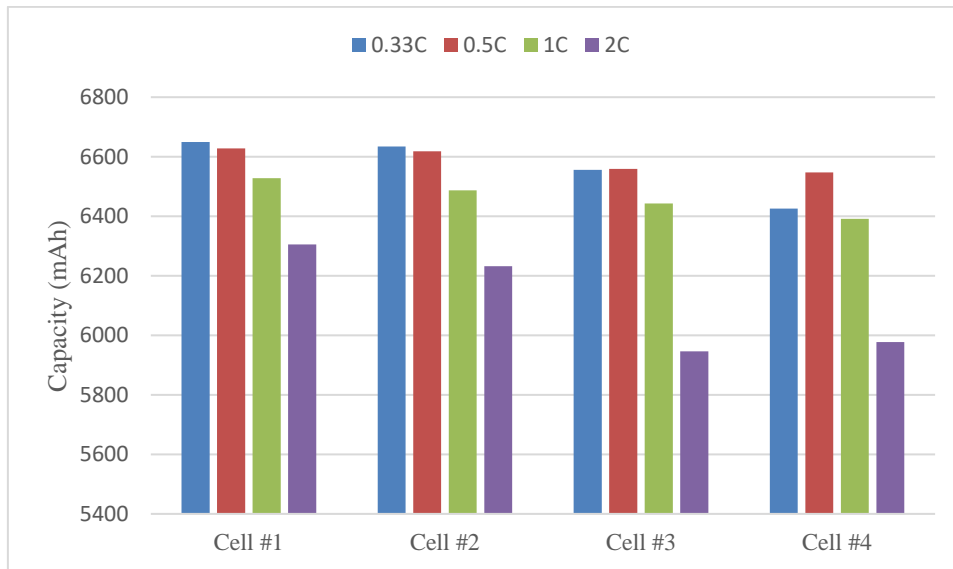


Fig. 8: Capacity test result in a clustered column chart for selected cells in different C_{rate} (Temperature 21°C)

Battery Pack Design

Generally with four different configurations as shown in Fig. 9 the cells can be connected in series and parallel to make the final battery pack according to the application requirements. In this figure, voltage monitoring in configurations c and d are much easier in comparison with configurations (a) and (b) for the BMS and also they have more flexibility, reliability, and redundancy [10].

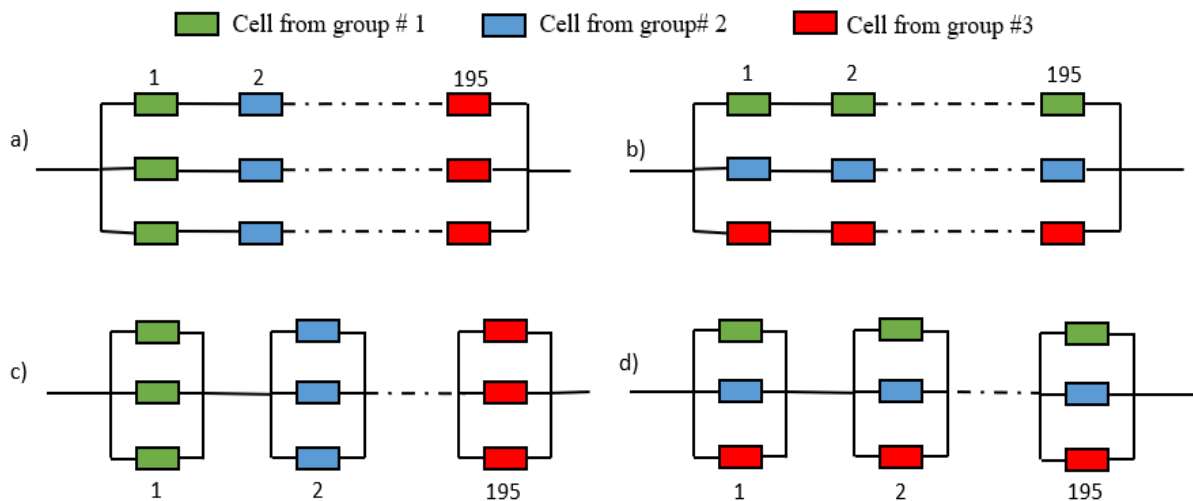


Fig. 9: Different configuration to make the battery pack according to the cell categorization

In parallel connection, there is the possibility of self-balancing, and cell to cell variation has less effect on pack performance [11]. Before assembling the final battery, two mini battery packs with configurations (c) and (d) have been made to evaluate the battery pack performance in two different configurations. The measurement results showed that the voltage balancing for the BMS is more challenging in configuration c, the strings with the weakest cells reached the cut-off voltage sooner than the strings with the best cells and the voltage disparity between the strings in configuration c is more than configuration d. Also, the battery capacity test as shown in Fig. 10 for two different configurations in different C_{rate} has been done to compare the performance of each configuration regarding their discharge capacity.

Finally to avoid impedance mismatching between the strings according to the cell categorization based on their internal impedance and to improve the battery pack performance by less voltage discrepancy between the strings, the configuration (d) has been selected.

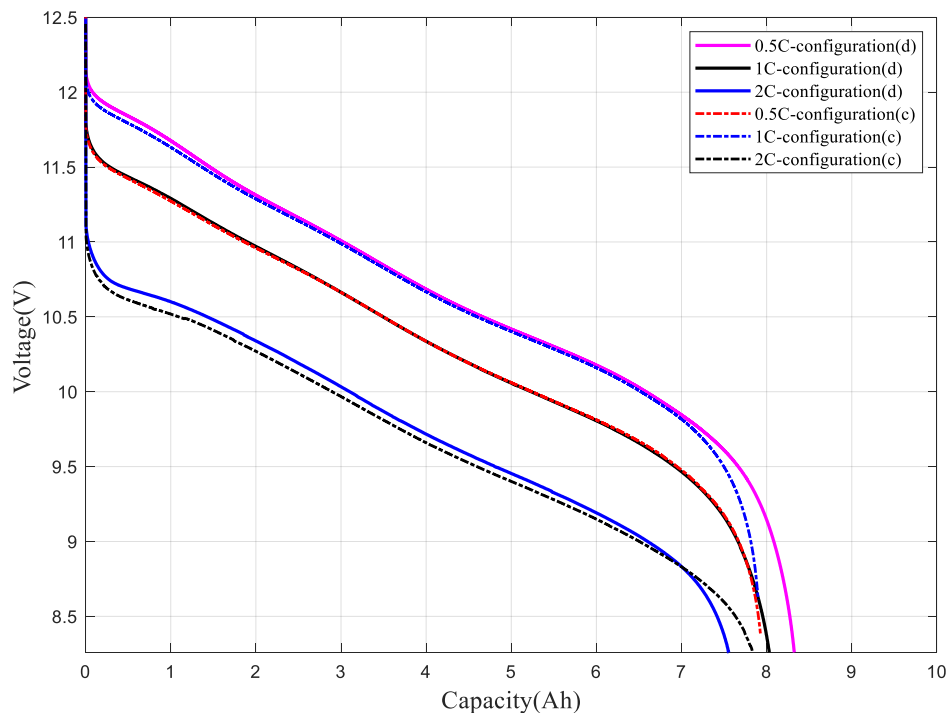


Fig. 10: Discharge capacity for two mini battery packs with configuration (c) and (d) with 10% discrepancy between the capacity of the cells

For each string, one cell from each group has been chosen in a way to match all equivalent parallel impedance of the strings. Fig. 11 illustrates the equivalent impedance for each string in configuration (d), the maximum deviation between the highest and lowest equivalent impedance in this configuration is only 0.0045 mΩ and the standard deviation is 0.0007 which means the equivalent impedance is very close to the mean.

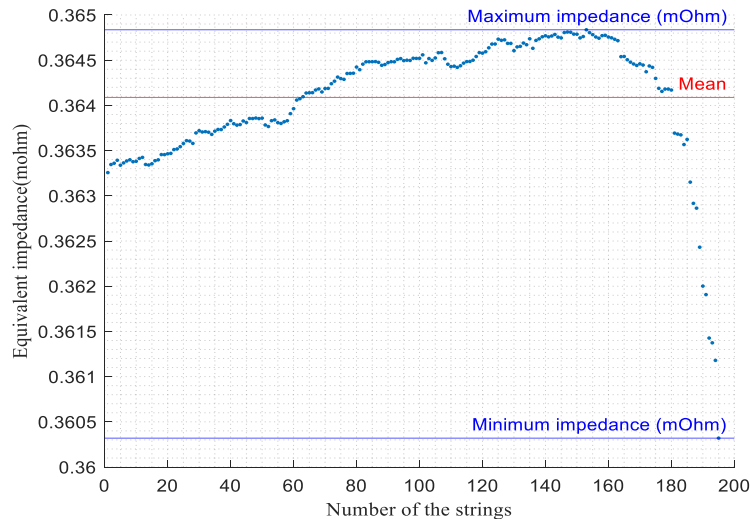


Fig. 11:Equivalent impedance of each string according to the (d) configuration

Conclusion

In this work to obtain the highest performance from the battery pack and considering this point that the cells with higher resistance have the lower capability to store the energy, battery electrochemical impedance spectroscopy have been used as the first tool to measure and analyze the impedance spectra for Li-Po cells and sort them according to their Nyquist plot. By applying the PEIS technique the cells are grouped into 4 segments based on the internal resistance, cells with the least resistance, marked as the best cells. It is observed that even the cells from the same batch from the same manufacturer are different in their parameters. There is a progressive increase in internal resistance in these segments with the best cells having the least and decent cells having the highest. To verify this technique that has been used to categorize the cells in the next step, one cell from each group has been selected, and by doing battery impulse current test and also battery capacity test the performance of each cell from each group has been tested. The results from the impulse current approach to obtain second-order model parameters and capacity test shows that most of the cells can satisfy their datasheet claim and the difference between the strongest and weakest cell in their capacity is 1.27% of the nominal capacity and the cells from the first group with less internal resistance have the best performance in battery capacity test and vice versa. As a result of the battery's complicated electrochemical dynamics, a discrepancy exists between performing the measurements on internal resistance by EIS and DC impulse approach due to the fact that all battery parameters depend on multiple factors and there is a real need for standardization of the tests for repeatability.

The final battery pack has been designed based on configuration (d) to avoid impedance mismatching between the strings, the standard deviation for the equivalent impedance of each string is close to zero ($\sigma=0.0007$) which means the equivalent impedances are very close to the mean. In regards to impedance uniformity between the strings, this configuration gives the best balance between the modules and finally for the battery pack. The impedance measurement for each module proves the impedance uniformity between the modules.

For future work, all different configurations will be compared based on the battery performance during the life-cycling and analyzing the battery lifetime.

References

- [1] B. Ferreira, "Batteries, the New Kids on the Block," *IEEE Power Electron. Mag.*, vol. 6, no. 4, pp. 32–34, Dec. 2019, doi: 10.1109/MPEL.2019.2947980.
- [2] Y. Ding, Z. P. Cano, A. Yu, J. Lu, and Z. Chen, "Automotive Li-Ion Batteries: Current Status and Future Perspectives," *Electrochem. Energy Rev.*, vol. 2, no. 1, pp. 1–28, 2019, doi: 10.1007/s41918-018-0022-z.
- [3] I. S. Kim, "A technique for estimating the state of health of lithium batteries through a dual-sliding-mode observer," *IEEE Trans. Power Electron.*, vol. 25, no. 4, pp. 1013–1022, 2010, doi: 10.1109/TPEL.2009.2034966.
- [4] O. Krishan and S. Suhag, "An updated review of energy storage systems: Classification and applications in distributed generation power systems incorporating renewable energy resources," *Int. J. Energy Res.*, vol. 43, no. 12, pp. 6171–6210, 2019, doi: 10.1002/er.4285.
- [5] P. Simon and Y. Gogotsi, "Materials for electrochemical capacitors," in *Nanoscience and Technology: A Collection of Reviews from Nature Journals*, World Scientific Publishing Co., 2009, pp. 320–329.
- [6] S. Muench, A. Wild, C. Friebe, B. Häupler, T. Janoschka, and U. S. Schubert, "Polymer-Based Organic Batteries," *Chem. Rev.*, vol. 116, no. 16, pp. 9438–9484, 2016, doi: 10.1021/acs.chemrev.6b00070.
- [7] Y. Liu, Y. G. Liao, and M. Lai, "Applications : Experiment , Modelling , and Validation," pp. 1–15, 2020.
- [8] G. Marin-Garcia, G. Vazquez-Guzman, J. M. Sosa, A. R. Lopez, P. R. Martinez-Rodriguez, and D. Langarica, "Battery Types and Electrical Models: A Review," *2020 IEEE Int. Autumn Meet. Power, Electron. Comput. ROPEC 2020*, no. Ropec, pp. 5–10, 2020, doi: 10.1109/ROPEC50909.2020.9258711.
- [9] W. Choi, H. C. Shin, J. M. Kim, J. Y. Choi, and W. S. Yoon, "Modeling and applications of electrochemical impedance spectroscopy (Eis) for lithium-ion batteries," *J. Electrochem. Sci. Technol.*, vol. 11, no. 1, pp. 1–13, 2020, doi: 10.33961/jecst.2019.00528.
- [10] D. Andrea, *Battery Management Systems for Large Lithium-ion Battery Packs*. Artech house, 2010.
- [11] M. Dubarry, C. Pastor-Fernández, G. Baure, T. F. Yu, W. D. Widanage, and J. Marco, "Battery energy storage system modeling: Investigation of intrinsic cell-to-cell variations," *J. Energy Storage*, vol. 23, no. December 2018, pp. 19–28, 2019, doi: 10.1016/j.est.2019.02.016.
- [12] Q. Wang, J. Wang, P. Zhao, J. Kang, F. Yan, and C. Du, "Correlation between the model accuracy and model-based SOC estimation," *Electrochim. Acta*, vol. 228, pp. 146–159, Feb. 2017, doi: 10.1016/j.electacta.2017.01.057.
- [13] Claudia Werckle, "IMPROVED EQUIVALENT-CIRCUIT MODELS OF LITHIUM-ION-IRON-PHOSPHATE CELLS," University of Colorado, Colorado, 2019.
- [14] B. Xia, X. Zhao, R. de Callafon, H. Garnier, T. Nguyen, and C. Mi, "Accurate Lithium-ion battery parameter estimation with continuous-time system identification methods," *Appl. Energy*, vol. 179, pp. 426–436, Oct. 2016, doi: 10.1016/j.apenergy.2016.07.005.
- [15] S. S. Madani, E. Schaltz, and S. Knudsen Kaer, "An Electrical Equivalent Circuit Model of a Lithium Titanate Oxide Battery," 2019, doi: 10.3390/batteries5010031.
- [16] A. I. Stroe, D. I. Stroe, M. Swierczynski, R. Teodorescu, and S. K. Kær, "Lithium-Ion battery dynamic model for wide range of operating conditions," *Proc. - 2017 Int. Conf. Optim. Electr. Electron. Equipment, OPTIM 2017 2017 Intl Aegean Conf. Electr. Mach. Power Electron. ACEMP 2017*, pp. 660–666, 2017, doi: 10.1109/OPTIM.2017.7975044.
- [17] Q. Sun, H. Zhang, J. Zhang, and W. Ma, "Adaptive unscented kalman filter with correntropy loss for robust state of charge estimation of lithium-ion battery," *Energies*, vol. 11, no. 11, 2018, doi: 10.3390/en11113123.